The electrometer concept and binding of cations to phospholipid bilayers

Andrea Catte,* Mykhailo Girych,† Matti Javanainen,‡ Markus S. Miettinen,§ Luca Monticelli,¶ Jukka Määttä,** Vasily S. Oganesyan,†† and O. H. Samuli Ollila‡‡

Despite of vast amount of experimental and theoretical studies, the binding affinity of cations, especially the biologically relevant Na^+ and Ca^{2+} ions, into a phosholipid bilayer is not agreed on in the literature. Here we directly compare the measured choline headgroup order parameters to the simulations with different models in the presence of different cations. We conclude that the simplest explanation for the experimental and theoretical observations is that at mM concentrations the Na^+ ions do not ~~penetrate into~~ bind to **1.Markus: 'penetrate into' gives the impression they go really deep, that is, even in the tails. On the other hand, 'bind to' could mean that they are bound just to the headgroup region. Should we maybe say precisely until where do they penetrate?** phosphatidylcholine lipid bilayers, in contrast to Ca^{2+}. Further, the binding affinity of Na^+ is overestimated in almost all molecular dynamics simulation models. However, the electrometer concept (connecting the choline order parameter changes to the amount of penetrating charge) is valid also in simulations.

This work has been, and continues to be, progressed and discussed through the blog: nmrlipids.blogspot.fi. Everyone is invited to join the discussion and make contributions through the blog. The manuscript will be eventually submitted to an appropriate scientific journal. Everyone who has contributed to the work through the blog will be offered coauthorship. For more details see: nmrlipids.blogspot.fi.

I. INTRODUCTION

The cation interactions with phospholipid membranes occur in a large amount of physiological processes, nerve cell signalling being the prime example. Thus, the interactions between different cations and phospholipid bilayers have been widely studied by experiments and theory. While it is practically agreed that the relative binding affinity of different ions follows the Hofmeister series [1–9], the quantitative binding affinities of different ions are not agreed on in the literature. The extensive reviews of the work done prior 1990 [2, 3] concluded that monovalent cations (Li^+ being an exception) interact only weakly with phospholipid bilayers, while for multivalent ions the interactions are significant. This conclusion has been supported by further studies where the bilayer properties have remained intact mM concentrations of monovalent salt [4, 10, 11]. On the other hand, the weak interactions with monovalent ions have been questioned in several experimental and molecular dynamics simulation studies [6–9, 12–18] suggesting stronger binding especially for Na^+ ions.

More specifically, mM concentrations NaCl has a negligible effect on the choline headgroup order parameters [19], area per molecule [10], dipole potential [20], and lipid lateral diffusion [11]; in contrast, these properties are significantly affected by the presense of $CaCl_2$ or other multivalent ions. In addition, water sorption isotherm for POPC/NaCl system was essentially similar to NaCl in pure water—indicating only weak interaction between ion and lipid [4]. Only minor changes in POPC infrared spectra were observed in the presense of NaCl compared to the significant changes in the presense of $CaCl_2$ and other multivalent ions, and it was again concluded that the Na^+-lipid interactions are weak [4].

In contrast, decrease of fluorescent probe rotational and translational dynamics in lipid bilayer with mM NaCl concentrations suggested significant Na^+ binding [7, 9, 12]. However, the reduced lateral diffusion is not observed in non-invasive NMR experiments, suggesting that fluorescence results arise from Na^+ interactions with probes rather than with lipids [11]. Also the interpretation of calorimetric measurements has been controversial: Previously the small effect of monovalent ions (except Li^+) on phase transition temperature compared to multivalent ions was interpreted such that only multivalent ions and Li^+ specifically bind to phosholipid bilayer [2], however, more recently the small changes in calorimetric experiments have been interpreted to indicate also Na^+ binding [8, 12]. In electrophoresis measurements of phosphatidylcholine vesicles, NaCl can increase the originally negative zeta potential close to zero, however, positive zeta potential can be typically reached only with multivalent ions or Lit^+ [1, 8, 14, 15, 21]. The lack of significant positive electrophoretic mobility in the presence of NaCl has been recognized to contradict with suggested strong binding of Na^+, however the contradiction has been explained by the effect of Cl^- ions to the electrophoretic mobility [22, 23]. Also changes in bilayer hardness and area per lipid measured with Atomistic Force Microscopy (AFM) are related to the Na+ binding to phospholipids [14–18].

In atomistic resolution molecular dynamics simulations, all the generally used models seems to predict binding of Na^+

* The authors are listed in alphaphetical order.; The author list is not completed.; University of East Anglia, Norwich, United Kingdom
† Helsinki Biophysics and Biomembrane Group, Department of Biomedical Engineering and Computational Science, Aalto University, Espoo, Finland
‡ Tampere University of Technology, Tampere, Finland
§ Fachbereich Physik, Freie Universität Berlin, Berlin, Germany
¶ Institut de Biologie et Chimie des Protéines (IBCP), CNRS UMR 5086, Lyon, France
** Aalto University, Espoo, Finland
†† University of East Anglia, Norwich, United Kingdom
‡‡ **Author to whom correspondence may be addressed. E-mail: samuli.ollila@aalto.fi.**; Helsinki Biophysics and Biomembrane Group, Department of Biomedical Engineering and Computational Science, Aalto University, Espoo, Finland

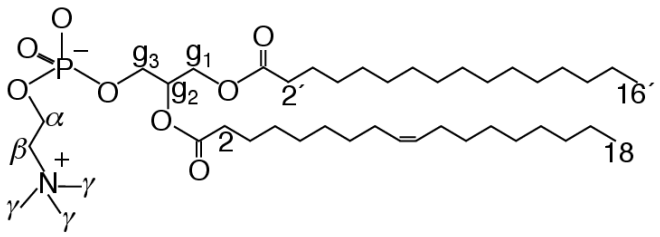

FIG. 1: Chemical structure of 1-palmitoyl-2-oleoylphosphatidylcholine (POPC).

ions into a phoshatidylcholine lipid bilayer, but the strength of binding depends on the model used [12, 13, 22, 24–27]. The reduced lipid lateral diffusion due to Na^+ binding in simulations agrees with fluorescent probe measurements [7, 9, 12], but not with the NMR experiments [11]. The area per lipid reduction due to Na^+ binding in simulations agrees with AFM experiments [14–18], however, the area reduction is observed at significantly too low concentrations when compared with the scattering experiments [10]. The simulations also predict too positive electrophoretic mobility with NaCl compared with experiments, however, this has been explained by the Cl^- ion behaviour [22, 23].

In this work, we resolve these contradictions by directly comparing the choline hydrocarbon segment order parameters, α and β in Fig. 1, between simulations and experiments as a function of NaCl and $CaCl_2$. According to the "electrometer concept" the changes of these order parameters can be used to measure the ion affinity to the phophatidylcholine lipid bilayer [19, 28–30]. Since the order parameters can be accurately measured from experiments and straightforwardly compared to simulations [**?**], the electrometer concept allows the direct comparison of binding affinity between simulations and experiments. In this work, we show that the qualitative response of order parameters to penetrating cations is qualitatively correct in simulations, but the Na+ affinity is significantly overestimated in several molecular dynamics simulation models. **2.Statement about Ca2+ to be added when we have the results.**

II. RESULTS AND DISCUSSION

The electrometer concept is based on the observed systematic absolute value increase for β and decrease for α segment order parameter with inceased cation binding and *vice versa* for anions [19, 28–30]. Only absolute values of the order parameters were measured in original experiments, while later experiments revealed that the order parameter is negative for β segment and positive for α segment [31–33]. Thus the both order parameter values are actually decreasing (becoming more negative) with bound cations [**?**]. The sign corrected choline order parameter changes for POPC and DPPC bilayers as a function NaCl and $CaCl_2$ concentrations, measured with H2 NMR [19, 28], are shown in Fig. 2. Only minute decreases are measured with NaCl while order of magnitude larger effect is observed with $CaCl_2$. Interpreted in terms of the electrometer concept, the result indicate negligible binding of monovalent Na^+ ions in constrast to multivalent Ca^{2+} ions [19, 28], in agreement with several other experimental studies [2–4, 10, 11]

Also order parameter changes with NaCl and $CaCl_2$ concentrations from various simulation models are shown in Fig. 2. The simulation details are in Table I and in Supplementary Information. The order parameter decrease with penetrating cations is observed in all simulation models in line with experiments. This indicates that the choline qualitative structural response can be reproduced in simulations despite of inaccuracies with varying severity in the choline and glycerol backbone structures, in agreement with our recent results with dehydration [34].

To study the correlation between order parameter changes and ion partitioning into a bilayer, suggested by the electrometer concept [19, 28–30], the ion density distributions from different simulation models as a function of membrane normal with NaCl and $CaCl_2$ are shown in Figs. 3 and 4, respectively. The density profiles from different models in Fig. 3 are arranged to increasing order according to the changes observed in order parameters with NaCl concentration in Fig. 2 such that the model with smallest change is on top and towards the bottom are models with larger observed order parameter changes. The Fig. 2 clearly shows that the larger Na^+ density peaks at the lipid bilayer interface are observed towards the bottom of the figure correlating with the increased order parameter change. Thus the Na^+ ion binding affinity is clearly related to the α and β order parameter changes in simulations are well, thus the electrometer concept [19, 28–30] can be used to compare the Na^+ ion binding affinity between simulations are experiments. This applies to all studied models despite of the varying quality of the sampled choline and glycerol backbone structures [34]. The Ca^{2+} penetration and related order parameter decrease is seen with all simulation models.

The smallest order parameter changes in best agreement with experiments with NaCl concentration are seen for the Orange, CHARMM36 and Lipid14 models in Fig.2. However, the ion density profiles in Fig. 3 show detectable differences in Na^+ affinity between these models, Orange having lowest affinity and CHARMM36 highest. None of the models reproduces all the order parameters in Fig. 2 within experimental error and these very small order parameter changes (less than 0.02) may be delicate to, e.g. initial structures. Thus we cannot conclude if one of these three models is more realistic than another, especially with physiological NaCl concentrations ($\sim$ 150mM) which is most relevant for most applications. On the other hand, all the other studied models clearly overestimate the choline order parameter changes respect to experiments, as

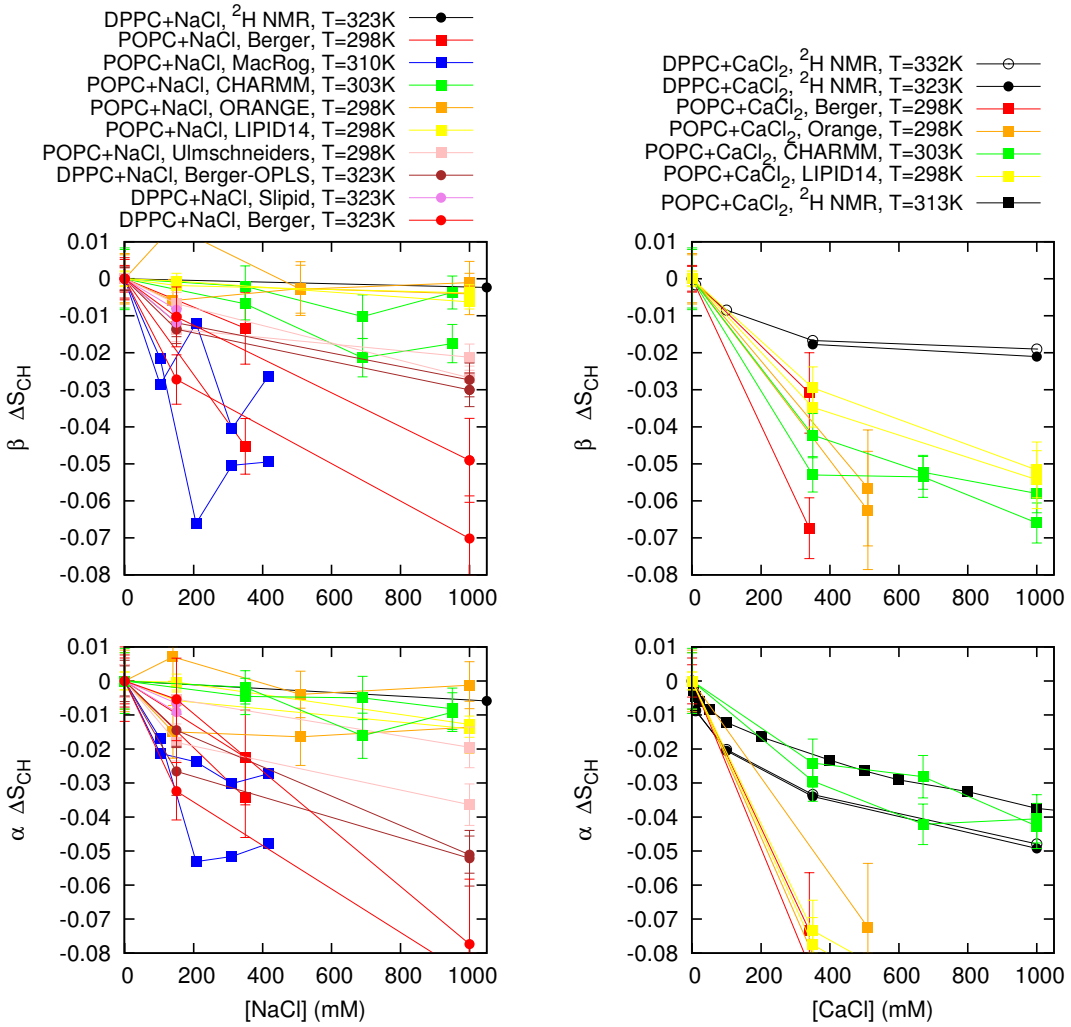

FIG. 2: The order parameter changes for β and α segments as a function of NaCl (left column) and $CaCl_2$ (right column) concentrations from simulations and experiments [19] (POPC with $CaCl_2$ from [28]). The signs of the experimental order parameters, taken from experiments without ions [31–33], can be assumed to be unchanged with concentrations represented here [28**?**]. It should be noted that none of the models used here reproduces the order parameters within experimental error for pure PC bilayer wihtout ions, indicating structural inaccuracies with varying severity for all models [34].

seen from Fig. 2. This is related to the unrealistically strong Na^+ binding to the bilayer, evidenced by the density peaks in Fig. 3 which are seen also with physiological concentrations.

It is agreed in the literature that the Ca^{2+} ions do penetrate in the phosphatidylcholine bilayer and significantly affect membrane properties already at mM concentrations of $CaCl_2$, however, the strength of the binding is not agreed on [13, 21, 28]. **4.Markus: Mention shortly what strengths have been suggested?** The binding and related order parameter decrease are seen in all tested models in Figs. 2 and 4. However, the order parameter changes are overestimated in all models in respect to the experiments, thus none of these models cannot be used to interpret the Ca^{2+} induced structural changes to the lipids or number of bound lipids. In contrast to the Na+, there is no clear correlation between Ca^{2+} binding affinity and order parameter changes, thus the overestimation of order parameter change can be due to, e.g. too strong strong binding, incorrect headgroup response to penetrating divalent cation or penetration depth. The penetration depth of Ca^{2+} ions is similar (density maxima close to ± 2 nm) in all models except Berger with deeper penetration depth (density maxima close to ± 1.8 nm). The location closer to water phase is probably more realistic since ^{1}H NMR and neutron scattering data indicates that Ca^{2+} interact mainly with choline group [2, 35–37]. Further, the ^{1}H NMR experiments suggest that the N-β-α-O dihedral is only in gaughe–conformation in the absense of ions, but in the presense of multivalent ions also anti–conformations would be present [36, 38]. However, since the models reproduce the conformations without ions with varying quality and the experimental order parameter response to $CaCl_2$ concentration current MD models cannot used to interpret this. **5.The P-N vector tilting analysis should be considered**

The most straightforward explanation for our results is that Na^+ ions do not practically penetrate into a PC lipid bilayer

TABLE I: Simulated lipid bilayers with ions. The ion concentrations are the concentration of ions in buffer to solute the lipid bilayers and calculated as [ion]=($N_{ion}\times$[water])/N_w, where [water]=55.5M. These correspond the concentrations reported in the experiments by Akutsu et al. [19].

Force field (lipid/ion)	lipid	[Ion] mM	[a]N_l	[b]N_w	[c]N_{Na}	[d]N_{Ca}	[e]N_{Cl}	[f]T (K)	[g]t_{sim}(ns)	[h]t_{anal} (ns)	Files
Berger-POPC-07[39]	POPC	0	128	7290	0	0	0	298	270	240	[40]
Berger-POPC-07[39]/Gromos [?]6.	POPC	340 (NaCl)	128	7202	44	0	44	298	110	50	[41]
Berger-POPC-07[39]/Gromos [?]7.	POPC	340 ($CaCl_2$)	128	7157	0	44	88	298	108	58	[42]
Berger-DPPC-98[43]	DPPC	0	72	2880	0	0	0	323	60	50	[44]
Berger-DPPC-98[43]/Gromos [?]	DPPC	0	72	2880	8	0	8	323	120	60	[45]
Berger-DPPC-98[43]/Gromos [?]	DPPC	1000 (NaCl)	72	2778	51	0	51	323	120	60	[46]
BergerOPLS-DPPC-06[47]	DPPC	0	72	2880	0	0	0	323	120	60	[48]
BergerOPLS-DPPC-06[47]/Åqvist [49]	DPPC	150	72	2880	8	0	8	323	120	60	[50]
BergerOPLS-DPPC-06[47]/Åqvist [49]	DPPC	1000	72	2778	51	0	51	323	120	60	[51]
CHARMM36[52]	POPC	0	72	2242	0	0	0	303	30	20	[53]
CHARMM36[52]/ionFF [54]	POPC	350 (NaCl)	72	2085	13	0	13	303	80	60	[55]
CHARMM36[52]/ionFF [54]	POPC	690 (NaCl)	72	2085	26	0	26	303	73	60	[56]
CHARMM36[52]/ionFF [54]	POPC	950 (NaCl)	72	2168	37	0	37	303	80	60	[57]
CHARMM36[52]/ionFF [?]	POPC	350 ($CaCl_2$)	128	6400	0	35	70	303	200	100	[58]
CHARMM36[52]/ionFF [?]	POPC	670 ($CaCl_2$)	128	6400	0	67	134	303	200	120	[59]
CHARMM36[52]/ionFF [?]	POPC	1000 ($CaCl_2$)	128	6400	0	100	200	303	200	100	[60]
MacRog[61]	POPC	0	288	14400	0	0	0	310	90	40	[62]
MacRog[61]/ionFF [?]8.	POPC	100 (NaCl)	288	14554	27	0	27	310	90	50	[63]
MacRog[61]/ionFF [?]9.	POPC	210 (NaCl)	288	14500	54	0	54	310	90	50	[63]
MacRog[61]/ionFF [?]10.	POPC	310 (NaCl)	288	14446	81	0	81	310	90	50	[63]
MacRog[61]/ionFF [?]11.	POPC	420 (NaCl)	288	14392	108	0	108	310	90	50	[63]
Orange, ionFF [?]	POPC	0	72	2880	0	0	0	298	60	50	[64]
Orange, ionFF [?]	POPC	140 (NaCl)	72	2866	7	0	7	298	120	100	[65]
Orange, ionFF [?]12.	POPC	510 (NaCl)	72	2802	26	0	26	298	120	100	[66]
Orange, ionFF [?]	POPC	1000 (NaCl)	72	2780	50	0	50	298	120	80	[67]
Orange, ionFF [?]13.	POPC	510 ($CaCl_2$)	72	2802	0	26	52	298	120	60	[68]
Slipid[69]	DPPC	0	128	3840	0	0	0	323	150	100	[70]
Slipid[69], ionFF [?]14.	DPPC	150 (NaCl)	600	18000	49	0	49	323	100	40	?
Lipid14/AMBER99SB-ILDN[?]	POPC	0	128	5120	0	0	0	298	205	200	[71]
Lipid14/AMBER99SB-ILDN[?]	POPC	150 (NaCl)	128	5120	12	0	12	298	205	200	[72]
Lipid14/AMBER99SB-ILDN[?]	POPC	1000 (NaCl)	128	5120	77	0	77	298	205	200	[73]
Lipid14/AMBER99SB-ILDN[?]	POPC	350 ($CaCl_2$)	128	6400	0	35	70	298	200	100	[74]
Lipid14/AMBER99SB-ILDN[?]	POPC	1000 ($CaCl_2$)	128	6400	0	100	200	298	200	100	[75]
Ulmschneiders/OPLS[?]	POPC	0	128	5120	0	0	0	298.15	205	200	[76]
Ulmschneiders/OPLS[?]	POPC	150 (NaCl)	128	5120	12	0	12	298.15	205	200	[77]
Ulmschneiders/OPLS[?]	POPC	1000 (NaCl)	128	5120	77	0	77	298.15	205	200	[78]

[a] The number of lipid molecules
[b] The number of water molecules
[c] The number of Na^+ molecules
[d] The number of Ca^{2+} molecules
[e] The number of Cl molecules
[f] Simulation temperature
[g] The total simulation time
[h] Time frames used in the analysis

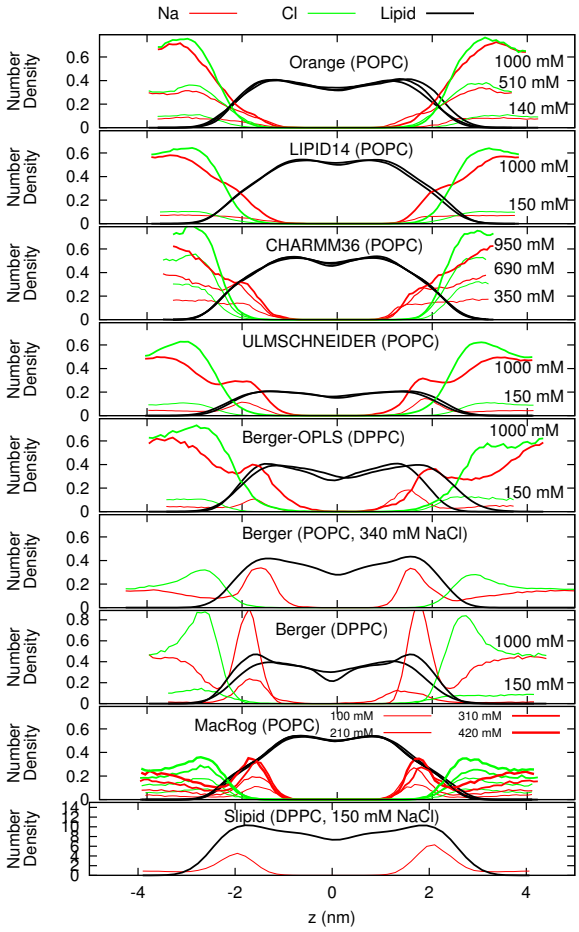

FIG. 3: Number density profiles for lipids, Na^+ and Cl^- ions from simulations with different force fields and different NaCl concetrations. The force fields are ordered according to the order parameter changes observed in Fig. 2 such that the models with smallest observed changes are top. The lipid densities are scaled with 100 (united atom) or 200 (all atom model) to make them visible with the used y-axis scale. Figure discussed in https://github.com/NMRLipids/lipid_ionINTERACTION/issues/4.

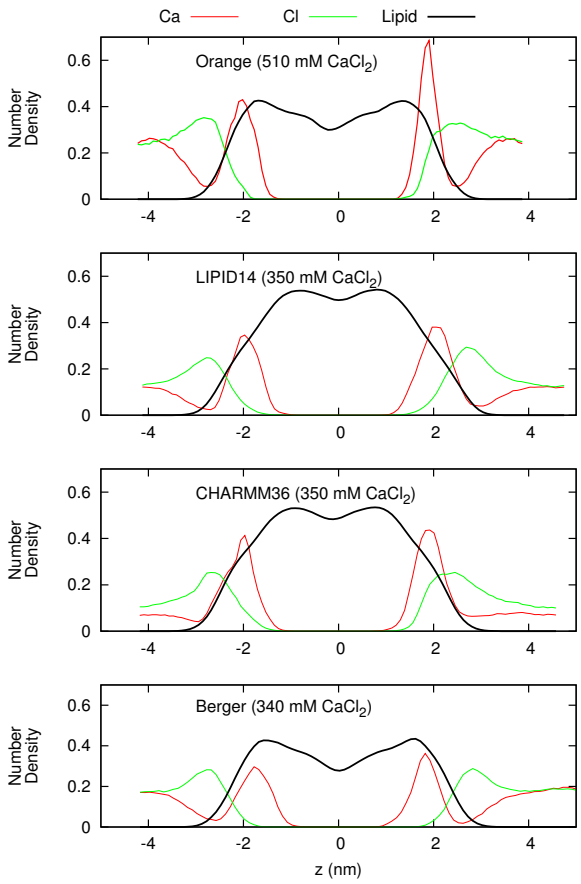

FIG. 4: Number density profiles for lipids, Ca^{2+} and Cl^- ions from simulations with different force fields. The profiles only with smallest available $CaCl_2$ concentration are shown for clarity. Figure including all the available concetrations is shown in the Supplementary Information. The lipid densities are scaled with 100 (united atom) or 200 (all atom model) to make them visible with the used y-axis scale. Figure discussed in https://github.com/NMRLipids/lipid_ionINTERACTION/issues/4.

3.We need compatible data for Slipids. This is easy to calculate by modifying the current scripts, if the data is available.

at mM concentrations, thus the presense of NaCl does not affect the bilayer properties as observed in various experiments [4, 10, 11, 19, 20, 28]. Consequently, the Na^+ penetration and concominant changes in order parameters, area per molecule and lateral diffusion seen in almost all simulation models would be artefact due to overestimated attraction between ions and lipid bilayer. Even though this would also explain the absense of positive zeta potential in electrophoresis experiments [1, 8, 14, 15, 21], the presented data do not rule out the suggested possibility of equal binding of Na^+ and Cl^- ions [23], however, this equal binding should happen in such a way that the bilayer properties are unaffected. The negligible binding of Na^+ at mM concentrations suggested here differs from the conclusions made from measurements of fluorescent probe dynamics [7, 9, 12], membrane hardness with AFM [14–18] and calorimetry [8, 12]. However, the fluorescent measurement results may arise from direct interactions between probe and ions, as already suggested by Filippov et al. [11]. Further, the calorimetric results have been also interpreted to support negligible binding [2], and AFM result is relatively indirect, thus there may be alternative explanations as well.

The origin for suggested inaccuracies in lipid-ion interactions in simulation models is unknown. In principle, the incorrect choline structure [34], lack of polarizability [79] or the used water model could cause such results. The effect of changes in lipid and ion models on the ion partitioning is discussed in the supplementary material. **15.In the Orange simulation only lipid model is changed, respect to Berger, and Jukka tested the effect of 0.7 charge scaling for Na ion (suggested by Leontyev et al. [79] to compensate to**

the lack of electronic polarizability in the model). I think we should discuss these things in supplementary material. Even though we cannot be fully conclusive, there is some essential information also in these results.

The failure of Gromos ions to properly account ion–ion and ion–water binding propensities of Na^+ and Cl^- ions has been reported previously [80]. The Åqvist ions have been parameterized in aqueous solutions with good agreement to experimental energies [81]. Yet, the binding affinity of ions to lipid bilayers has not been calibrated—instead it is assumed to work based purely on forces obtained using combination rules. Compared to Gromos ions, Åqvist parameters are better, yet Na^+ overbinding still occurs.

III. CONCLUSIONS

We have compared phosholipid bilayer interactions with NaCl and $CaCl_2$ between different molecular dynamics simulation models and ^{2}H NMR experiments. The comparison led to the following conclusions

- The electrometer concept suggesting connection between α and β order parameter decrease and cation partitioning [19, 28–30] works also in simulations, despite of inaccuracies in actual atomistic resolution structures.

- The most straighforward explanation for the various experimental observations is that there is no Na^+ ion binding into the phospholipid bilayer at mM concentrations, in constrast to Ca^{2+} which specifically binds.

- The Na^+ partitioning is overestimated in almost all molecular dynamics simulation models, however, from the publicly available models the CHARMM36 has the most realistic description.

- **16.Final conclusions about the structural response to be written once we have all the results**

This work has been, and will be, progressed and discussed through the blog: nmrlipids.blogspot.fi. Everyone is invited to join the discussion and make contributions through the blog. The manuscript will be eventually submitted to an appropriate scientific journal. Everyone who has contributed to the work through the blog will be offered coauthorship. For more details see: nmrlipids.blogspot.fi.

Acknowledgements: OHSO acknowledges Tiago Ferreira for very useful discussions, the Emil Aaltonen foundation for financial support, Aalto Science-IT project and CSC-IT Center for Science for computational resources. MSM acknowledges financial support from the Volkswagen Foundation (86110).

SUPPLEMENTARY INFORMATION

Appendix A: Effect of ion model and polarization

We also tested if different ion models and implicit accounting of polarization would affect ion binding. To compensate the missing electronic polarizability, Leontyev et al. [79] have suggested that ion charges should be scaled by a factor of 0.7. To test if this scaling alone could correct the ion binding affinity we ran simulations with scaled ion charges with Berger-DPPC-98 and BergerOPLS-DPPC-06 models (the systems identical as in Table I except that the ion charges are scaled with 0.7, the files available at [82–85]). The order parameter changes and ion affinity are smaller with scaled charges but yet overestimated respect to the experiments as seen from Figs. 5 and 6. Thus the overestimated binding affinity cannot be fixed by only scaling charges.

Appendix B: Structural changes induced by $CaCl_2$

Appendix C: methods

1. Simulated systems

All simulations are ran with a standard setup for planar lipid bilayer in zero tension with periodic boundary conditions with Gromacs software package (version numbers 4.5-X-5.0.X).

2. Simulation details

a. Berger

The simulation without ions is the same as in [34]. The starting structures for simulations with ions is made by replacing water molecules with appropriate amount of ions under study. **17.Samuli, finalize and check the methods.**

The Berger force field was used for the POPC [86], with the dihedral potential next to the double bond taken from [87]. The simulations are identical to previous publications [39, 88, 89]. Timestep of 2 fs was used with leap-frog integrator. Covalent bond lengths were constrained with LINCS algorithm [90, 91]. Coordinates were written every 10 ps. PME with real space cut-off 1.0 nm was used for electrostatics. Plain cut-off was used for the Lennard-Jones interactions with a 1.0 nm cut-off. The neighbour list was updated every 5th step with cut-off 1.0 nm. Temperature was coupled separately for lipids and water to 298 K with the velocity-rescale method [92] with coupling constant 0.1 ps^{-1}. Pressure was semi-isotropically coupled to the athmospheric pressure with the Berendsen method [93].

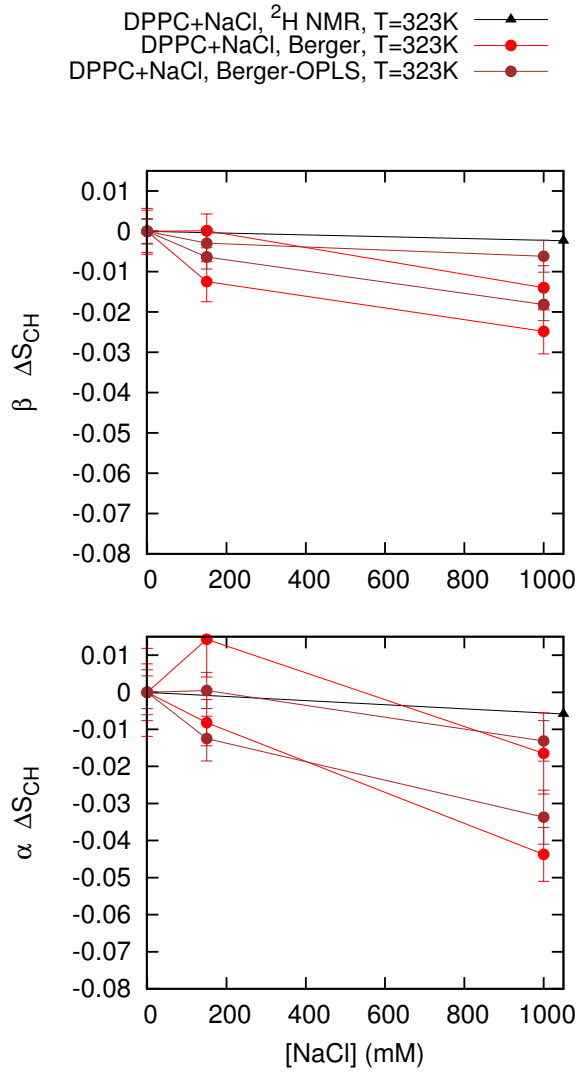

FIG. 5: Order parameter changes in scaled and non-scaled models. The Berger-OPLS compatible model results are missing since there are no results without ions for this.

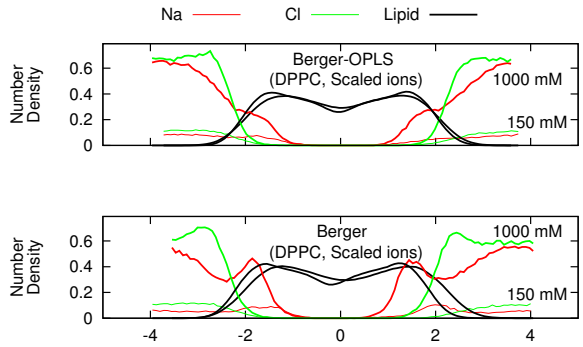

FIG. 6: Number density profiles for lipids, Na^+ and Cl^- ions from simulations with different force fields and different NaCl concetrations. The ion charges are scaled with 0.7 to compensate the missing electronic polarizability [79]. The lipid densities are scaled with 100 (united atom) or 200 (all atom model) to make them visible with the used y-axis scale.

b. BergerOPLS

18.Simulation details from Jukka Määttä

c. CHARMM36

POPC with NaCl The simulation without ions is taken directly from [34, 53]. The starting structures for simulations with NaCl were made by replacing randomly located water molecules of the structure of pure POPC simulation with appropriate amount of ions. The force field for lipid were the same as in [34, 53]. The ion parameters with NBFIX by Venable et al. [54] were used. Simulations were ran with Gromacs 4.5.5 software [94]. **19.Still to be checked** Timestep of 1 fs was used with leap-frog integrator. Covalent bonds with hydrogens were constrained with LINCS algorithm [90, 91]. Coordinates were written every 5 ps. PME with real space cut-off 1.4 nm was used for electrostatics. Lennard-Jones interactions were switched to zero between 0.8 nm and 1.2 nm. The neighbour list was updated every 5th step with cut-off 1.4 nm. Temperature was coupled separately for lipids and water to 303 K with the velocity-rescale method [92] with coupling constant 0.2 ps. Pressure was semi-isotropically coupled to the athmospheric pressure with the Berendsen method [93].

POPC with $CaCl_2$ The starting structures with varying amounts of $CaCl_2$ ions were constructed using the CHARMM-GUI Membrane Builder (http://www.charmm-gui.org/) online tool [95]. All runs were performed with Gromacs 5.0.3 software package [96] and CHARMM36 additive force field parameters for lipids [52] and ions [**?**] were obtained from CHARMM-GUI input files. Standard CHARMM-GUI mdp options were used. Particularly, h-bond lengths were constrained with LINCS [90, 91]. The temperatures of the lipids and the solvent were separately coupled to the Nose-Hoover [97, 98] thermostat with a target temperature of 303 K and a relaxation time constant of 1.0 ps. Semi-isotropical pressure coupling to 1 bar was obtained with the Parrinello-Rahman barostat [99] with a time constant of 5 ps. Equations of motion were integrated with the Verlet algorithm [100] using a timestep of 2 fs. Long-range electrostatic interactions were calculated using the PME [101, 102] method with a fourth order smoothing spline. A real space cut-off of 1.2 nm was employed with grid spacing of 0.12 nm in the reciprocal space. Lennard-Jones interactions were smoothly swithced to zero between 1.0 nm and 1.2 nm. Verlet cutoff-scheme [100] were used with the long-range neighbor list updated every 20 steps. Coordinates were written every 10 ps. After energy minimization and an equilibration run of 0.5 ns, 200ns simulations were ran and the last 100ns of each simu-

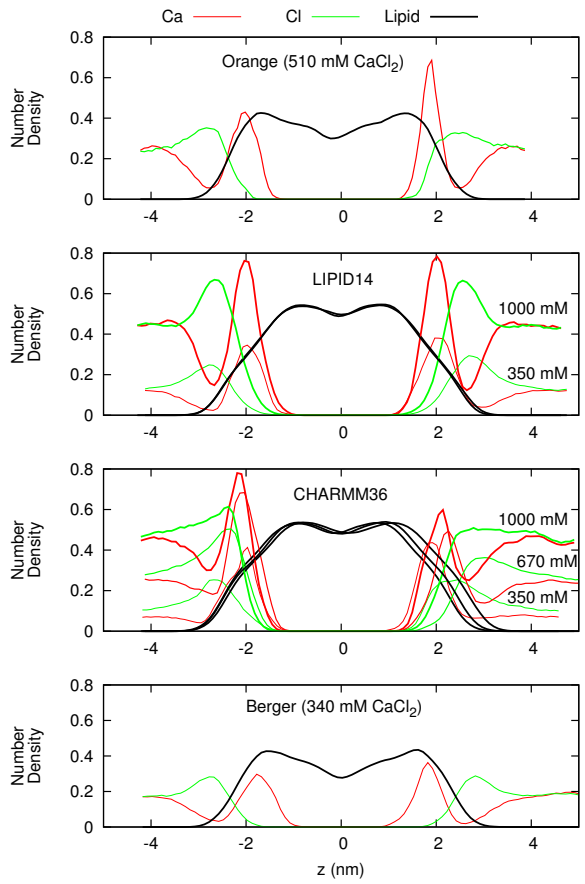

FIG. 7: Number density profiles for lipids, Ca^{2+} and Cl^{-} ions from simulations with different force fields and different $CaCl_2$ concentrations. The lipid densities are scaled with 100 (united atom) or 200 (all atom model) to make them visible with the used y-axis scale. Figure discussed in https://github.com/NMRLipids/lipid_ionINTERACTION/issues/4

lation was employed for the analysis.

d. *MacRog*

The simulation parameters are identical to those employed in our earlier study [34] for the full hydration and dehydration simulations. The initial structures with varying amounts of NaCl were constructed from an extensively hydrated bilayer by replacing water molecules with ions using the Gromacs tool genion [103]. Even at the highest considered salt concentration, the amount of water molecules per lipid after this replacement process was still greater than 50.

e. *Orange*

20.Jukka Maatta and Luca Monticelli, please deliver as much details as you can.

f. *Slipids*

The simulation without ions is the same as in [34].

21.Add references to Slipids with ions. For the simulations with ions, the starting DPPC lipid bilayer, which was built with the online CHARMM-GUI (http://www.charmm-gui.org/), contained 600 lipids, 30 water molecules/lipid, Na^{+} and Cl^{-} ions (150 mM NaCl). The TIP3P water model was used to solvate the system. All-atom MD simulations of DPPC lipid bilayers were performed at ten different temperatures (283, 298, 303, 308, 312, 313, 314, 318, 323, and 333 K) using the GROMACS software package version 4.5.5 [94] and the Stockholm lipids (Slipids) force field parameters for phospholipids. After energy minimization and a short equilibration run of 50 ps (time step 1 fs), 100 ns production runs were performed using a time step of 2 fs with leap-frog integrator. All covalent bonds were constrained with the LINCS algorithm. Coordinates were written every 100 ps. PME with real space cut-off at 1.0 nm was used for Coulomb interactions. Lennard-Jones interactions were switched to zero between 1.0 nm and 1.4 nm. The neighbour lists were updated every 10^{th} step with a cut-off of 1.6 nm. Temperature was coupled separately for upper and bottom leaflets of the lipid bilayer, and for water to one of the temperatures reported above with the Nosé-Hoover thermostat using a time constant of 0.5 ps. Pressure was semi-isotropically coupled to the atmospheric pressure with the Parrinello-Rahman barostat using a time constant of 10 ps. The last 40 ns of each simulation was employed for the analysis of DPPC choline and glycerol backbone order parameters.

g. *Lipid14*

The starting structures with varying amounts of ions were constructed using the CHARMM-GUI Membrane Builder (http://www.charmm-gui.org/) online tool [95]. The GROMACS compatible force field parameters generated in [34] and available at [104] were used. The TIP3P water model [105] was used to solvate the system. Ions were described by AMBER99SB-ILDN force field [**?**]. All runs were performed with Gromacs 5.0.3 software package [96] and LIPID14 force field parameters for POPC [106].

H-bond lengths were constrained with LINCS [90, 91]. The temperatures of the lipids and the solvent were separately coupled to the Nose-Hoover [97, 98] thermostat with a target temperature of 298.15 K and a relaxation time constant of 0.1 ps. Semi-isotropical pressure coupling to 1 bar was obtained with the Parrinello-Rahman barostat [99] with a time constant of 2 ps. Equations of motion were integrated with the Verlet algorithm [100] using a timestep of 2 fs. Long-range electrostatic interactions were calculated using the PME [101, 102] method with a fourth order smoothing spline. A real space cut-off of 1.0 nm was employed with grid spacing of 0.12 nm in the reciprocal space. Lennard-Jones potentials were cut-off at 1 nm, with a dispersion correction applied to both energy and pressure. Verlet cutoff-scheme [100] were used with the long-range neighbor list updated every 20 steps. Coordinates

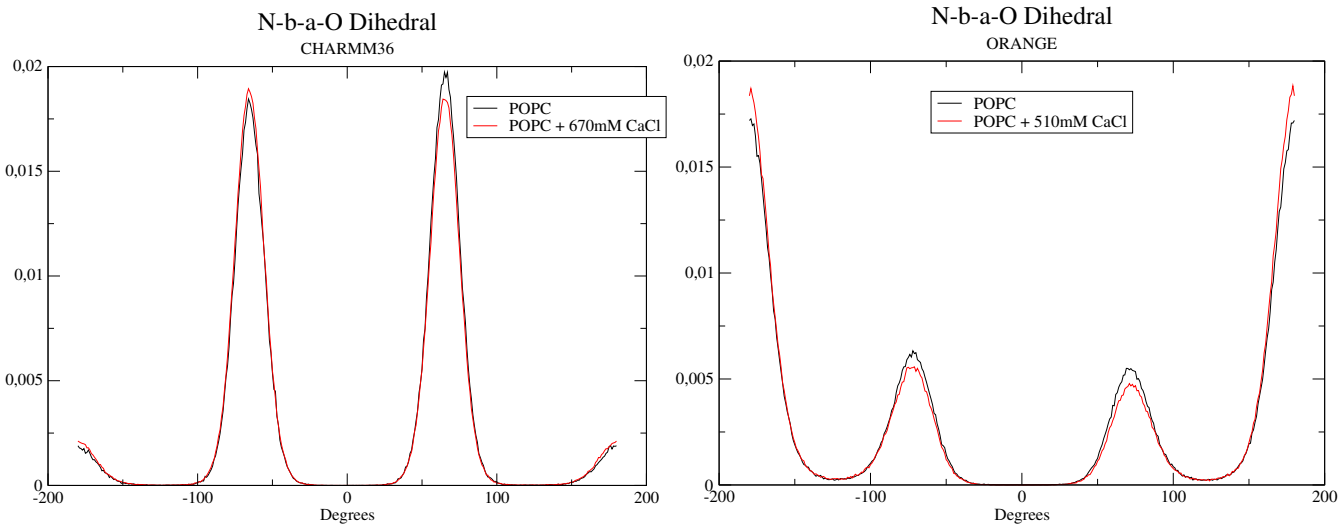

FIG. 8: Dihedral angle distributions for O-β-α-N dihedral with different $CaCl_2$ concentrations.

were written every 10 ps.

After energy minimization and an equilibration run of 5 ns, 200ns production runs were performed and analysed. In case of the CaCl2 systems only the last 100ns of each simulation was employed for the analysis.

h. Ulmscneiders

The starting structures with varying amounts of ions were constructed using the CHARMM-GUI Membrane Builder (http://www.charmm-gui.org/) online tool [95]. The force field parameters were obtained from Lipidbook [107]. The TIP3P water model [105] was used to solvate the system. Additionally, the simulations of ion-free bilayer were repeated with both Verlet and Group cutoff-schemes [76]. There was no significant difference in headgroup or glycerol backbone order parameters between these cutoff-schemes. All runs were performed with Gromacs 5.0.3 software package [96]. The glycerol backbone order parameters without iones were not the same as reported in the previous study [34]. The origin of discrepancy was located to the different initial structures which was taken from CHARMM-GUI in this work and from Lipidbook in the previous work. Since the order parameters with the initial structure from CHARMM-GUI are closer to the experimental values, the results indicate that the structure available from Lipidbook is stuck to a state with incorrect glycerol backbone strucuture, for more discussion see `https://github.com/NMRLipids/lipid_ionINTERACTION/issues/8`.

All-bond lengths were constrained with LINCS [90, 91]. The temperatures of the lipids and the solvent were separately coupled to the Nose-Hoover [97, 98] thermostat with a target temperature of 298.15 K and a relaxation time constant of 0.1 ps. Semi-isotropical pressure coupling to 1 bar was obtained with the Parrinello-Rahman barostat [99] with a time constant of 2 ps. Equations of motion were integrated with the Verlet algorithm [100] using a timestep of 2 fs. Long-range electrostatic interactions were calculated using the PME [101, 102] method with a fourth order smoothing spline. A real space cut-off of 1.0 nm was employed with grid spacing of 0.12 nm in the reciprocal space. Lennard-Jones potentials were cut-off at 1 nm, with a dispersion correction applied to both energy and pressure. Verlet cutoff-scheme [100] were used with the long-range neighbor list updated every 20 steps. Coordinates were written every 10 ps. After energy minimization and an equilibration run of 5 ns, 200ns simulations were ran and the last 100ns of each simulation was employed for the analysis.

3. Analysis

The order parameters were calculated from simulation trajectories directly applying the equation $S_{\mathrm{CH}} = \langle \frac{3}{2}\cos^2\theta - \frac{1}{2} \rangle$, where θ is the angle between a given C–H bond and the bilayer normal. For united atom models the hydrogen locations were regenerated for each molecule in each frame after the simulation trajectory was created. ??The statistical error estimate for each order parameter calculated from simulation was roughly 0.01, which is much smaller than the differences discussed in this work.?? **22.Markus: What do the question marks mean? Was the error estimation not performed yet?**

TODO

P.

1. Markus: 'penetrate into' gives the impression they go really deep, that is, even in the tails. On the other hand, 'bind to' could mean that they are bound just to the headgroup region. Should we maybe say precisely until where do they penetrate? 1

---

[1] M. Eisenberg, T. Gresalfi, T. Riccio, and S. McLaughlin, Biochemistry **18**, 5213 (1979).
[2] G. Cevc, Biochim. Biophys. Acta - Rev. Biomemb. **1031**, 311 (1990).
[3] J.-F. Tocanne and J. Teissi, Biochimica et Biophysica Acta (BBA) - Reviews on Biomembranes **1031**, 111 (1990).
[4] H. Binder and O. Zschörnig, Chem. Phys. Lipids **115**, 39 (2002).
[5] J. J. Garcia-Celma, L. Hatahet, W. Kunz, and K. Fendler, Langmuir **23**, 10074 (2007).
[6] E. Leontidis and A. Aroti, The Journal of Physical Chemistry B **113**, 1460 (2009).
[7] R. Vacha, S. W. I. Siu, M. Petrov, R. A. Böckmann, J. Barucha-Kraszewska, P. Jurkiewicz, M. Hof, M. L. Berkowitz, and P. Jungwirth, J. Phys. Chem. A **113**, 7235 (2009).
[8] B. Klasczyk, V. Knecht, R. Lipowsky, and R. Dimova, Langmuir **26**, 18951 (2010).
[9] F. F. Harb and B. Tinland, Langmuir **29**, 5540 (2013).
[10] G. Pabst, A. Hodzic, J. Strancar, S. Danner, M. Rappolt, and P. Laggner, Biophys. J. **93**, 2688 (2007).
[11] A. Filippov, G. Ordd, and G. Lindblom, Chemistry and Physics of Lipids **159**, 81 (2009).
[12] R. A. Böckmann, A. Hac, T. Heimburg, and H. Grubmüller, Biophys. J. **85**, 1647 (2003).
[13] R. A. Böckmann and H. Grubmüller, Ang. Chem. Int. Ed. **43**, 1021 (2004).
[14] S. Garcia-Manyes, G. Oncins, and F. Sanz, Biophys. J. **89**, 1812 (2005).
[15] S. Garcia-Manyes, G. Oncins, and F. Sanz, Electrochimica Acta **51**, 5029 (2006), ISSN 0013-4686, bioelectrochemistry 2005 Bioelectrochemistry 2005, URL http://www.sciencedirect.com/science/article/pii/S0013468606002775.
[16] T. Fukuma, M. J. Higgins, and S. P. Jarvis, Phys. Rev. Lett. **98**, 106101 (2007).
[17] U. Ferber, G. Kaggwa, and S. Jarvis, European Biophysics Journal **40**, 329 (2011), ISSN 0175-7571, URL http://dx.doi.org/10.1007/s00249-010-0650-7.
[18] L. Redondo-Morata, G. Oncins, and F. Sanz, Biophysical Journal **102**, 66 (2012).
[19] H. Akutsu and J. Seelig, Biochemistry **20**, 7366 (1981).
[20] R. J. Clarke and C. Lpfert, Biophysical Journal **76**, 2614 (1999).
[21] S. A. TATULIAN, European Journal of Biochemistry **170**, 413 (1987), ISSN 1432-1033, URL http://dx.doi.org/10.1111/j.1432-1033.1987.tb13715.x.
[22] M. L. Berkowitz, D. L. Bostick, and S. Pandit, Chem. Rev. **106**, 1527 (2006).
[23] V. Knecht and B. Klasczyk, Biophys. J. **104**, 818 (2013).
[24] J. N. Sachs, H. Nanda, H. I. Petrache, and T. B. Woolf, Biophys. J. **86**, 3772 (2004).
[25] A. Cordomi, O. Edholm, and J. J. Perez, J. Chem. Theo. Comput. **5**, 2125 (2009).
[26] C. Valley, J. Perlmutter, A. Braun, and J. Sachs, J. Membr. Biol. **244**, 35 (2011).
[27] M. L. Berkowitz and R. Vacha, Acc. Chem. Res. **45**, 74 (2012).
[28] C. Altenbach and J. Seelig, Biochemistry **23**, 3913 (1984).
[29] J. Seelig, P. M. MacDonald, and P. G. Scherer, Biochemistry **26**, 7535 (1987).

[30] P. G. Scherer and J. Seelig, Biochemistry **28**, 7720 (1989).
[31] M. Hong, K. Schmidt-Rohr, and A. Pines, Journal of the American Chemical Society **117**, 3310 (1995).
[32] M. Hong, K. Schmidt-Rohr, and D. Nanz, Biophysical Journal **69**, 1939 (1995).
[33] J. D. Gross, D. E. Warschawski, and R. G. Griffin, Journal of the American Chemical Society **119**, 796 (1997).
[34] A. Botan, A. Catte, F. Favela, P. Fuchs, M. Javanainen, W. Kulig, A. Lamberg, M. S. Miettinen, L. Monticelli, J. Määttä, et al., *Towards atomistic resolution structure of phosphatidylcholine glycerol backbone and choline headgroup at different ambient conditions*, http://arxiv.org/abs/1309.2131v2 (2015), nMRlipids project, nmrlipids.blogspot.fi, 1309.2131.
[35] H. Hauser, M. C. Phillips, B. Levine, and R. Williams, Nature **261**, 390 (1976).
[36] H. Hauser, W. Guyer, B. Levine, P. Skrabal, and R. Williams, Biochimica et Biophysica Acta (BBA) - Biomembranes **508**, 450 (1978), ISSN 0005-2736, URL http://www.sciencedirect.com/science/article/pii/0005273678900913.
[37] L. Herbette, C. Napolitano, and R. McDaniel, Biophysical Journal **46**, 677 (1984).
[38] H. Hauser, W. Guyer, and F. Paltauf, Chemistry and Physics of Lipids **29**, 103 (1981).
[39] S. Ollila, M. T. Hyvönen, and I. Vattulainen, J. Phys. Chem. B **111**, 3139 (2007).
[40] O. H. S. Ollila, T. Ferreira, and D. Topgaard (2014), URL {http://dx.doi.org/10.5281/zenodo.13279}.
[41] O. O. H. Samuli, *MD simulation trajectory and related files for POPC bilayer with 340mM NaCl (Berger model delivered by Tieleman, ffgmx ions, Gromacs 4.5)* (2015), URL http://dx.doi.org/10.5281/zenodo.32144.
[42] O. O. H. Samuli, *MD simulation trajectory and related files for POPC bilayer with 340mM CaCl_2 (Berger model delivered by Tieleman, ffgmx ions, Gromacs 4.5)* (2015), URL http://dx.doi.org/10.5281/zenodo.32173.
[43] S.-J. Marrink, O. Berger, P. Tieleman, and F. Jähnig, Biophysical Journal **74**, 931 (1998).
[44] J. Määttä (2015), URL {http://dx.doi.org/10.5281/zenodo.13934}.
[45] J. Mtt, *Dppc_berger_nacl* (2015), URL http://dx.doi.org/10.5281/zenodo.16319.
[46] J. Määttä, *Dppc_berger_nacl_1mol* (2015), URL http://dx.doi.org/10.5281/zenodo.17210.
[47] D. P. Tieleman, J. L. MacCallum, W. L. Ash, C. Kandt, Z. Xu, and L. Monticelli, J. Phys. Condens. Matter **18**, S1221 (2006).
[48] J. Määttä, *Dppc_berger_opls06* (2015), URL http://dx.doi.org/10.5281/zenodo.17237.
[49] J. Åqvist, The Journal of Physical Chemistry **94**, 8021 (1990).
[50] J. Määttä, *Dppc_berger_opls06_nacl* (2015), URL http://dx.doi.org/10.5281/zenodo.16484.
[51] J. Määttä, *Dppc_berger_opls06_nacl_1mol* (2015), URL http://dx.doi.org/10.5281/zenodo.17208.
[52] J. B. Klauda, R. M. Venable, J. A. Freites, J. W. O'Connor, D. J. Tobias, C. Mondragon-Ramirez, I. Vorobyov, A. D. M. Jr, and R. W. Pastor, J. Phys. Chem. B **114**, 7830 (2010).
[53] O. O. H. Samuli and M. Miettinen (2015), URL {http://dx.doi.org/10.5281/zenodo.13944}.
[54] R. M. Venable, Y. Luo, K. Gawrisch, B. Roux, and R. W. Pastor, The Journal of Physical Chemistry B **117**, 10183 (2013).
[55] S. Ollila, *MD simulation trajectory and related files for POPC bilayer with 350mM NaCl (CHARMM36, Gromacs 4.5)* (2015), URL http://dx.doi.org/10.5281/zenodo.32496.
[56] S. Ollila, *MD simulation trajectory and related files for POPC bilayer with 690mM NaCl (CHARMM36, Gromacs 4.5)* (2015), URL http://dx.doi.org/10.5281/zenodo.32497.
[57] S. Ollila, *MD simulation trajectory and related files for POPC bilayer with 950mM NaCl (CHARMM36, Gromacs 4.5)* (2015), URL http://dx.doi.org/10.5281/zenodo.32498.
[58] G. Mykhailo and O. O. H. Samuli, *Popc_charmm36_cacl2_035mol* (2015), URL http://dx.doi.org/10.5281/zenodo.35159.
[59] G. Mykhailo and O. O. H. Samuli, *Popc_charmm36_cacl2_067mol* (2015), URL http://dx.doi.org/10.5281/zenodo.35160.
[60] G. Mykhailo and O. O. H. Samuli, *Popc_charmm36_cacl2_1mol* (2015), URL http://dx.doi.org/10.5281/zenodo.35156.
[61] A. Maciejewski, M. Pasenkiewicz-Gierula, O. Cramariuc, I. Vattulainen, and T. Rog, The Journal of Physical Chemistry B **118**, 4571 (2014).
[62] M. Javanainen (2014), URL {http://dx.doi.org/10.5281/zenodo.13498}.
[63] M. Javanainen, *POPC @ 310K, varying amounts of NaCl. Model by Maciejewski and Rog* (2015), URL http://dx.doi.org/10.5281/zenodo.14976.
[64] O. H. S. Ollila, J. Mtt, and L. Monticelli, *MD simulation trajectory for POPC bilayer (Orange, Gromacs 4.5.)* (2015), URL http://dx.doi.org/10.5281/zenodo.34488.
[65] O. H. S. Ollila, J. Mtt, and L. Monticelli, *MD simulation trajectory for POPC bilayer with 140mM NaCl (Orange, Gromacs 4.5.)* (2015), URL http://dx.doi.org/10.5281/zenodo.34491.
[66] O. H. S. Ollila, J. Mtt, and L. Monticelli, *MD simulation trajectory for POPC bilayer with 510mM NaCl (Orange, Gromacs 4.5.)* (2015), URL http://dx.doi.org/10.5281/zenodo.34490.
[67] S. Ollila, J. Mtt, and L. Monticelli, *MD simulation trajectory for POPC bilayer with 1000mM NaCl (Orange, Gromacs 4.5.)* (2015), URL http://dx.doi.org/10.5281/zenodo.34497.
[68] O. H. S. Ollila, J. Mtt, and L. Monticelli, *MD simulation trajectory for POPC bilayer with 510mM CaCl_2 (Orange, Gromacs 4.5.)* (2015), URL http://dx.doi.org/10.5281/zenodo.34498.
[69] J. P. M. Jämbeck and A. P. Lyubartsev, The Journal of Physical Chemistry B **116**, 3164 (2012).
[70] J. Määttä (2014), URL {http://dx.doi.org/10.5281/zenodo.13287}.
[71] M. Girych and O. H. S. Ollila, *Popc_amber_lipid14_verlet* (2015), URL http://dx.doi.org/10.5281/zenodo.30898.
[72] M. Girych and O. H. S. Ollila, *Popc_amber_lipid14_nacl_015mol* (2015), URL http://dx.doi.org/10.5281/zenodo.30891.
[73] M. Girych and O. H. S. Ollila, *Popc_amber_lipid14_nacl_1mol* (2015), URL http://dx.doi.org/10.5281/zenodo.30865.
[74] G. Mykhailo and O. O. H. Samuli, *Popc_amber_lipid14_cacl2_035mol* (2015), URL http://dx.doi.org/10.5281/zenodo.34415.

[75] G. Mykhailo and O. O. H. Samuli, *Popc_amber_lipid14_cacl2_1mol* (2015), URL http://dx.doi.org/10.5281/zenodo.35074.

[76] M. Girych and O. H. S. Ollila, *Popc_ulmschneider_opls_verlet_group* (2015), URL http://dx.doi.org/10.5281/zenodo.30904.

[77] M. Girych and O. H. S. Ollila, *Popc_ulmschneider_opls_nacl_015mol* (2015), URL http://dx.doi.org/10.5281/zenodo.30892.

[78] M. Girych and O. H. S. Ollila, *Popc_ulmschneider_opls_nacl_1mol* (2015), URL http://dx.doi.org/10.5281/zenodo.30894.

[79] I. Leontyev and A. Stuchebrukhov, Phys. Chem. Chem. Phys. **13**, 2613 (2011).

[80] M. M. Reif, M. Winger, and C. Oostenbrink, Journal of Chemical Theory and Computation **9**, 1247 (2013), pMID: 23418406, http://dx.doi.org/10.1021/ct300874c, URL http://dx.doi.org/10.1021/ct300874c.

[81] J. Aaqvist, The Journal of Physical Chemistry **94**, 8021 (1990), http://dx.doi.org/10.1021/j100384a009, URL http://dx.doi.org/10.1021/j100384a009.

[82] J. Määttä (2015), URL {http://dx.doi.org/10.5281/zenodo.16320}.

[83] J. Määttä, *Dppc_berger_nacl_1mol_scaled* (2015), URL http://dx.doi.org/10.5281/zenodo.17228.

[84] J. Määttä (2015), URL {http://dx.doi.org/10.5281/zenodo.16485}.

[85] J. Mtt, *Dppc_berger_opls06_nacl_1mol_scaled* (2015), URL http://dx.doi.org/10.5281/zenodo.17209.

[86] O. Berger, O. Edholm, and F. Jähnig, Biophys. J. **72**, 2002 (1997).

[87] M. Bachar, P. Brunelle, D. P. Tieleman, and A. Rauk, J. Phys. Chem. B **108**, 7170 (2004).

[88] T. M. Ferreira, F. Coreta-Gomes, O. H. S. Ollila, M. J. Moreno, W. L. C. Vaz, and D. Topgaard, Phys. Chem. Chem. Phys. **15**, 1976 (2013).

[89] T. M. Ferreira, O. H. S. Ollila, R. Pigliapochi, A. P. Dabkowska, and D. Topgaard, The Journal of Chemical Physics **142**, 044905 (2015), URL http://scitation.aip.org/content/aip/journal/jcp/142/4/10.1063/1.4906274.

[90] B. Hess, H. Bekker, H. J. C. Berendsen, and J. G. E. M. Fraaije, J. Comput. Chem. **18**, 1463 (1997).

[91] B. Hess, Journal of Chemical Theory and Computation **4**, 116 (2008).

[92] G. Bussi, D. Donadio, and M. Parrinello, The Journal of Chemical Physics **126** (2007).

[93] H. J. C. Berendsen, J. P. M. Postma, W. F. van Gunsteren, A. DiNola, and J. R. Haak, J. Chem. Phys. **81**, 3684 (1984).

[94] S. Pronk, S. Pll, R. Schulz, P. Larsson, P. Bjelkmar, R. Apostolov, M. R. Shirts, J. C. Smith, P. M. Kasson, D. van der Spoel, et al., Bioinformatics **29**, 845 (2013).

[95] J. Lee, X. Cheng, J. M. Swails, M. S. Yeom, P. K. Eastman, J. A. Lemkul, S. Wei, J. Buckner, J. C. Jeong, Y. Qi, et al., Journal of Chemical Theory and Computation **0**, null (0).

[96] M. J. Abraham, T. Murtola, R. Schulz, S. Pll, J. C. Smith, B. Hess, and E. Lindahl, SoftwareX **12**, 19 (2015), ISSN 2352-7110, URL http://www.sciencedirect.com/science/article/pii/S2352711015000059.

[97] S. Nose, Mol. Phys. **52**, 255 (1984).

[98] W. G. Hoover, Phys. Rev. A **31**, 1695 (1985).

[99] M. Parrinello and A. Rahman, J. Appl. Phys. **52**, 7182 (1981).

[100] S. Pll and B. Hess, Computer Physics Communications **184**, 2641 (2013), ISSN 0010-4655, URL http://www.sciencedirect.com/science/article/pii/S0010465513001975.

[101] T. Darden, D. York, and L. Pedersen, The Journal of Chemical Physics **98** (1993).

[102] U. L. Essman, M. L. Perera, M. L. Berkowitz, T. Larden, H. Lee, and L. G. Pedersen, J. Chem. Phys. **103**, 8577 (1995).

[103] M. Abraham, D. van der Spoel, E. Lindahl, B. Hess, and the GROMACS development team, *GROMACS user manual version 5.0.7* (2015), URL www.gromacs.org.

[104] O. H. S. Ollila and M. Retegan, *Md simulation trajectory and related files for popc bilayer (lipid14, gromacs 4.5)* (2014), URL http://dx.doi.org/10.5281/zenodo.12767.

[105] W. L. Jorgensen, J. Chandrasekhar, J. D. Madura, R. W. Impey, and M. L. Klein, The Journal of Chemical Physics **79** (1983).

[106] C. J. Dickson, B. D. Madej, . A. Skjevik, R. M. Betz, K. Teigen, I. R. Gould, and R. C. Walker, Journal of Chemical Theory and Computation **10**, 865 (2014).

[107] J. Domaski, P. Stansfeld, M. Sansom, and O. Beckstein, The Journal of Membrane Biology **236**, 255 (2010), ISSN 0022-2631.